Journal of Applied Research and Technology

www.jart.icat.unam.mx

Journal of Applied Research and Technology 21 (2023) 433-446

Original

Heavy metals and sulfate removal from acid mine drainage using steel mill slag in a rotational mixing device

C. R. Blanco-Zúñiga[a] • C. N. Orjuela-Fajardo[a] • N. Rojas-Arias[a,b]*

[a]*Universidad Pedagógica y Tecnológica de Colombia.*
Avenida Central del Norte 39-115 - P.O. Box 150001, Boyacá, Colombia
[b]*Federal University of São Carlos, Graduate Program in Materials Science and Engineering,*
Rod. Washington Luiz Km 235 SP-310, 13565-905, São Carlos, Brazil

Received 12 03 2021; accepted 05 02 2022
Available 06 30 2023

Abstract: The steel mill slag (SMS) production in converter furnaces is one of the main by-products generated during steel production. This waste material is usually composed of different metal oxides that include basic cations such Ca, Mn, and Mg. These cations can favor alkalinity and heavy metals removal when they are partially dissolved in a contaminant solution such as acid mine drainage (AMD). This work aims to study the potential use of SMS produced in converter furnaces in the mining-steel region of Boyacá- Colombia as an alternative to pre-treat AMD produced by coal mining in the zone. The SMS were separated into two particle sizes by screening, and these were put in contact with AMD samples in a rotational mixing system for 36 hours. The pH, total Fe (Fe^{2+}, $^{3+}$), SO_4^{2-}, and heavy metals concentration were analyzed at 0, 12, 24 and 36 hours' time intervals. The results show that SMS produced in the region is an optimal low-cost alternative to treat AMD, allowing complete heavy metals removal in the first 12 hours of treatment. Furthermore, Fe and SO_4^{2-} removal were observed, reaching 99.9 % and 85 %, respectively, at 36 hours. The application of rotational mixing allows complete mixing between AMD and SMS, reducing the possible precipitates adhesion on the surface, limiting the reactivity losses. This mixing treatment device favors continuous use, avoiding the application of cleaning stages that could be required in the future for optimal functioning.

Keywords: Steel mill slag, acid mine drainage (AMD), heavy metals, sulfates and total Fe, rotational mixing device

*Corresponding author.
E-mail address: nicolas.rojas@estudante.ufscar.br (N. Rojas-Arias).
Peer Review under the responsibility of Universidad Nacional Autónoma de México.

1. Introduction

Post-mining impacts on a region's water resources are a topic of global concern. Acid mine drainage (AMD) is one of the by-products generated during these processes. It is characterized by a high heavy metals and sulfates concentration and a pH < 4.5 that can lead to the basins degradation and other water sources and the biota and fauna that are harbored in them (Bwapwa et al., 2017; Luptáková et al., 2016; Rambabu et al., 2020; Skousen et al., 2017).

The pyrite (FeS_2) oxidation contained within the mineral compounds, e.g. during the coal mining, is the principal acidification source producing AMD (Dold, 2014; Silva et al., 2020). The contact of pyrite with atmospheric oxygen (O_2) and water (H_2O) favors the release of large amounts of protonic acidity (H^+) and SO_4^{2-}, lowering the pH of the medium (Skousen et al., 2000; Tabelin et al., 2017; Wolfe, 2015). The increase in acidity allows the solubilization of other metals contained in the mine, such as As, Cu, Ni, Zn Co, and Cr (Clyde et al., 2016; Kobielska et al., 2018; Masindi, Gitari, et al., 2017; Núñez-Gómez et al., 2019), which makes AMD treatment or reuse difficult due to the need for additional processes (Masindi, Osman, & Abu-Mahfouz, 2017). The presence and concentration of these elements will depend mainly on the geo-genesis of the zone and the mineral compounds composition that produces the AMD (Obreque-Contreras et al., 2015).

In Colombia, coal mining is one of the principal mining activities, being the largest producer in Latin America and one of the primary exporters worldwide (Prieto & Duitama, 2004). The Department of Boyacá is one of the primary producers of coal in Colombia. This mineral is necessary for energy and steel production industries situated in the area; therefore, the need to mitigate the negative impacts generated by the AMD, besides other secondary waste produced during mining processes in the zone, has become an issue of great importance (Silva et al., 2020).

AMD can be treated by passive and active systems. These technologies utilize one or a combination of chemical, physical and biological processes, including pH control which is the most common process for AMD remediation. Passive systems are used in acidity conditions of 800 mg $CaCO_3 \cdot L^{-1}$ or less, flow rates under $50 L \cdot s^{-1}$, and low acidity loads (<100-150 kg $CaCO_3$/day). Within the passive systems, the most representative are: oxic-anoxic limestone drains, aerobic-anaerobic wetlands, reducing and alkalinity producing systems, and permeable reactive barriers.

The active systems are not limited by operational parameters, and they can be designed to carry out the AMD treatment under several acidity and metal load conditions (Taylor et al., 2005). The slag beds are also considered a passive system for AMD treatment, and their use depends on the chemical characterization. The neutralization potential (NP) of steel slags ranges from 45 to 78 %, and the main property of this raw material is the non-absorption of CO_2 from the air and convert back to relatively insoluble limestone. In general, steel slag can produce more alkalinity than equal weights of limestone (from 500 to 2000 $mg \cdot L^{-1}$, compared to 60 to 80 $mg \cdot L^{-1}$). The alkalinity generated comes from CaO and tri-calcium silicate minerals and it depends on particle size and contact time (Ziemkiewicz & Skousen, 1999). Steel-slag leach bed (SLB) are designed to treat 1000g acidity $t^{-1} \cdot day^{-1}$ (Skousen & Ziemkiewicz, 2005).

The application of steel mill slag (SMS) produced in some steelmaking stages, such as the conversion of pig iron into steel through converter furnaces, has been presented as an excellent raw material to replace part of the materials used in the construction of road infrastructures (Masindi, Osman & Abu-Mahfouz, 2017; Tiwari et al., 2016), and concrete production (Jeong et al., 2016). However, these SMS can also generate alkaline leachates through their interaction with climate and water conditions. In such a manner, improper storage can cause negative impacts on the environment (Król et al., 2020; Van der Sloot & Van Zomeren, 2012). The ability of SMS produced in steelmaking processes to generate highly basic leachates has focused the interest in the application of this by-product for its use in the treatment of AMD, allowing the removal of dissolved heavy metals and sulfates, as well as an increase in the pH of the solution, as reported by Masindi et al. (2020).

The high worldwide steel market demand represents a significant increase in slag production, making its utilization unavoidable. There is also a need for reuse and to give value to all these wastes in the mining-environmental sector. The proximity between the steel industry and the coal mining and stockpiles in the Boyacá region can reduce the costs generated by SMS transportation and the SMS that can take advantage as an alternative for AMD treatment. Therefore, this work studied the effect of the application of SMS produced in converter furnaces used in steel production on the treatment of AMD produced in the region of Boyacá, Colombia. The tests were carried out in a rotational mixing device at low revolutions; the effect of the SMS particle size was observed during the AMD samples treatment.

2. Experimental

2.1. Precautions to avoid sample contamination.

In order to avoid sample contamination, AMD samples were collected in glass containers, which were hermetically sealed. The containers were previously washed with distilled and deionized water by ultrasound repeatedly to eliminate any contaminant in them. This process was also performed on the vessel used in the rotational mixing device. The tests were carried out in controlled environments at a laboratory scale, previously adapted under ISO 14644. The laboratory's

operating personnel had the necessary safety and protection equipment during the handling of reagents and raw materials to avoid possible contamination of the samples.

2.2. Raw material

2.2.1. AMD

AMD samples produced by coal washing were extracted from coal stockpile companies located in the region of Paipa-Boyacá, Colombia. The AMD samples were collected following the procedure reported by the Institute of Hydrology, Meteorology and Environmental Studies - IDEAM Code: M-S-LC-I004 (IDEAM, 2020). The AMD physicochemical analysis was focused mainly on the determination of pH (SCHOTT Handylab pH-11 pH meter), conductivity (SCHOTT Handylab conductivity meter), dissolved oxygen (DO) (Winkler method - SCHOTT Handylab LF12 conductivity meter), SO_4^{2-} (SM4500-SO_4^{2-} turbidimetric method) and; total iron (Fe^{2+}, Fe^{3+}) (SM3500 Fe-B Spectroquant® Multy colorimetric method). Heavy metals such as $As^{3+,\ 5+}$, Cd^{2+}, and Pb^{2+} were determined by voltammetry, using HM-500 TRACE2O metaware equipment. According to the geographic location of these coal companies, a high amount of AMD is generated due to the high precipitation rates in the region (IDEAM, 2018). The maximum daily precipitation values were obtained during October (sample collection period), favoring a higher degree of dissolution and transport of metals and sulfates contained in the ore.

2.2.2. BOF-converter slags

The SMS samples produced during the conversion of pig-iron into steel using a basic-oxygen-furnace were obtained from the integrated steel plant located in Paz del Rio - Boyacá, Colombia. The SMS was reduced in size using a Blake-type jaw crusher and then washed with distilled and deionized water to remove possible impurities. The drying stage was carried out in an electric oven at 105 °C for 24 hrs. to eliminate the moisture retained. The SMS dried samples were subjected to granulometric analysis stages, according to the ASTM E-11/95 standard. The granulometric curve obtained is shown in Fig. 1.

The SMS was separated according to two specific particle sizes ranging from 4.75 mm to 2.0 mm (Type I) and between 2 mm and 0.3 mm (Type II). Size separation was performed to evaluate any variation in the SMS chemical composition and its effect during the treatment of AMD. The chemical composition of SMS was determined by X-ray fluorescence (XRF) tests on samples extracted according to ASTM D75-03. The relative density and water absorption percentage tests were determined according to INVE E 222-13 standard, using samples of crushed SMS with a particle size of less than 4.75 mm. The relative density test calculates the volume occupied by the material or aggregate based on an absolute volume. The absorption test represents a change in aggregate mass as a function of the amount of water absorbed by the permeable pores of its particles concerning the mass in dry conditions.

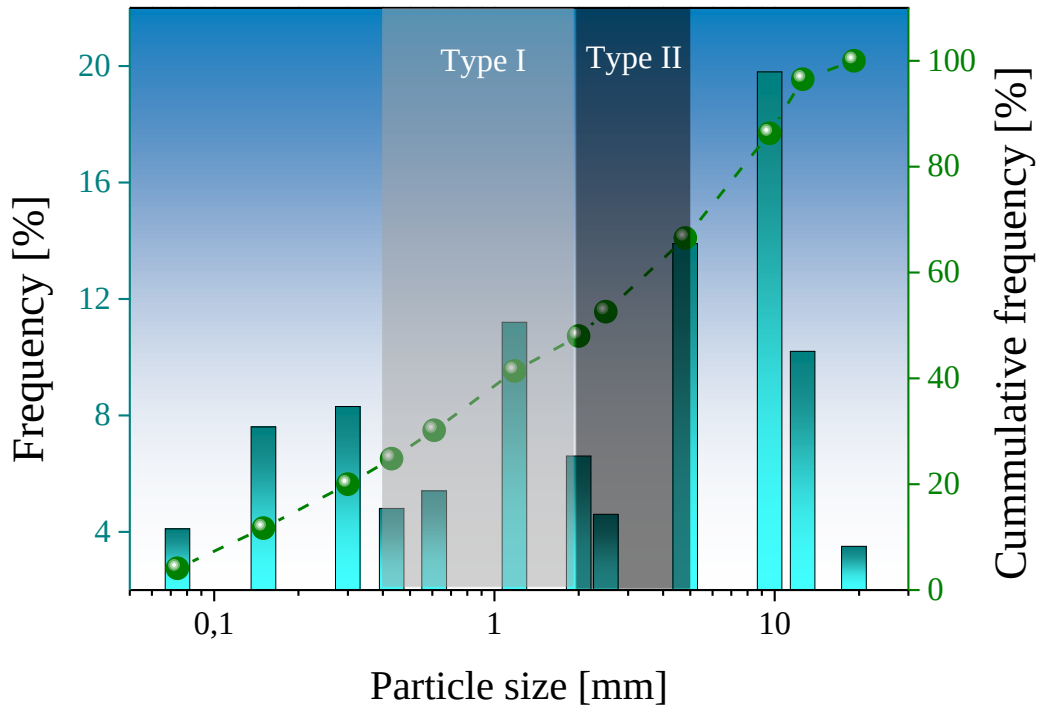

Fig. 1. SMS curve of particle size distribution. Particle size ranges for SMS samples are shaded light gray (for Type I) and dark gray (for Type II). Particle sizes below or above this range were neglected in this study.

2.3. Mechanical rotational mixing device

The rotational mixing device used in this work consisted of hermetically sealed cylindrical glass vessels with a capacity of 1 L, placed on rotating rollers. The complete system was powered by an AC motor, controlling the rotational speed at 6RPM using a digital tachometer Cybertech DT6236B. The scheme of this device is presented in Fig. 2. Low rotation speeds allowed a homogeneous agitation of the mixture, favoring the contact of SMS particles with AMD. On the other hand, the continuous agitation allows an interaction between the SMS particles generating abrasion or wear processes, keeping the reactivity.

The glass vessels were filled with 700 mL of AMD and 140 g of one of the previously selected types of SMS. The 5:1 ratio was performed according to that reported by Name and Sheridan (2014). Three replicates' tests were performed for each of the two types of SMS used for a total of 6 trials. The mixture was subjected to a continuous rotation, extracting samples in triplicate for pH, total Fe, and SO_4^{2-} analysis at time intervals of 12, 24, and 36 hours, obtaining a total of 54 samples in the six trials performed. Subsequently, the AMD treated samples were filtered to remove the total suspended solids (TSS) present in the fluid. The SMS used in this work were dried at 105 °C for 24 hours for XRF analysis. For all-purpose, the results are presented as the average of the processed data.

3. Results and discussion

3.1. Raw material characterization

3.1.1. AMD samples

Table I shows the physicochemical parameters of the AMD used in this work. As seen, AMD presents a high concentration of SO_4^{2-} and total Fe, characteristic of this type of drainage and the presence of heavy metals such as $As^{3+,\ 5+}$, Cd^{2+}, and Pb^{2+} (Skousen et al., 2019; Vasquez & Escobar, 2020). A highly acidic pH is observed, set at pH = 2.25; additionally, the deficiency of DO (dissolved oxygen) allows cataloging the AMD as a hypoxic/anoxic fluid associated possibly with Fe^{2+} concentrations higher than 63 mg·L^{-1}, which is capable of depleting the oxygen content in the AMD (Hustwit et al., 1992). In this work, metallic species of ferrous iron (Fe^{2+}) and ferric iron (Fe^{3+}) were not quantified separately.

The characterization of the AMD samples shows that the concentrations of pH, sulfates, Total Fe, $As^{3+,\ 5+}$, and Cd^{2+} exceed the values established by Colombian Resolution 631 of 2015, (Resolución 631 de 2015. Ministerio de Medio Ambiente y Desarrollo Sostenible - Colombia., 2105), The As content is 50 times higher than permitted, while the Fe content values exceed the limit value by more than 2700X. The high Fe ion content is due to the high pyrite content present in coal ores in the region, which in contact with O_2, H_2O, and even iron-oxidizing bacteria and sulfates, favors the formation of Fe^{2+}, $Fe^{3+}{}_{(aq)}$, sulfates, and proton acidity in the form of $H^+{}_{(aq)}$, generated from the following reactions (Akinwekomi et al., 2017; Hallberg, 2010; Masindi, 2016):

$$2FeS_{2(s)} + 7O_{2(g)} + 2H_2O \rightarrow 2Fe^{2+}_{(aq)} + 4H^+_{(aq)} + 4SO^{2-}_{4(aq)} \quad (1)$$

$$4Fe^{2+}_{(aq)} + O_{2(g)} + 4H^+_{(aq)} \rightarrow 4Fe^{3+}_{(aq)} + 2H_2O_l \quad (2)$$

$$FeS_{2(s)} + 14Fe^{3+} + 8H_2O \rightarrow 15Fe^{2+} + 2SO^{2-}_{4(l)} + 16H^+ \quad (3)$$

$$Fe^{3+}_{(aq)} + 3H_2O_l \rightarrow Fe(OH)_{3(s)} + 3H^+_{(aq)} \quad (4)$$

Likewise, sulfate and Cd concentrations are slightly higher than the permitted concentration. Pb^{2+} present in the AMD is the only metal whose value is below the limit established in the resolution, so it is not susceptible to treatment (removal by precipitation).

3.1.2. SMS samples

The Type I and Type II slag samples obtained during the crushing and screening stages presented average specific gravity values of 2.92 ± 0.48 g·cm^{-3} and an absorption percentage of 11.37 %. Apparent density values between 3.1 – 3.6 g·cm^{-3} have been reported in the literature (Bing et al., 2019; Thomas et al., 2019). The absorption percentage of this material represents the amount of water that can be trapped in the pores, established as a mass. Although there is no relationship between this parameter and surface area, steel mill slag is considered to have a large surface area (Bing et al., 2019), which increases with decreasing particle size and can influence particle reactivity, as in the case of limestone (Maree & Plessis, 1993). The SMS surface area was not calculated in this work due to the variation in particle size even after the screening process.

Fig. 3 presents the elemental chemical composition of Type I and Type II SMS. The values were established from the percentage of constituent elements. The presence of significant elements that make up the slag, such as Ca, Si, Fe, Mg, and Al, is usually associated with mineralogical species in the form of oxides, e.g., CaO, SiO_2 FeO MgO_2, and Al_2O_3 (Name & Sheridan, 2014). Both types of SMS show a similar composition, with a high Ca content, close to 40 %, which favors the basicity of the slag. Type II samples show a 4% higher Fe content, while Si, Al, Mg, and Mn contents tend to be slightly lower. This behavior is comparable to fine and coarse particulates used in mining and iron and steel processes (Rojas Arias et al., 2018). The majority percentages presence of the elements Ca, Mn, and Mg allows the presence of cations that contribute to alkalinity generation in fluids. Several authors have also reported these elements as the main components of slags (Aziz et al., 2014; Belhadj et al., 2012; Masindi et al., 2018).

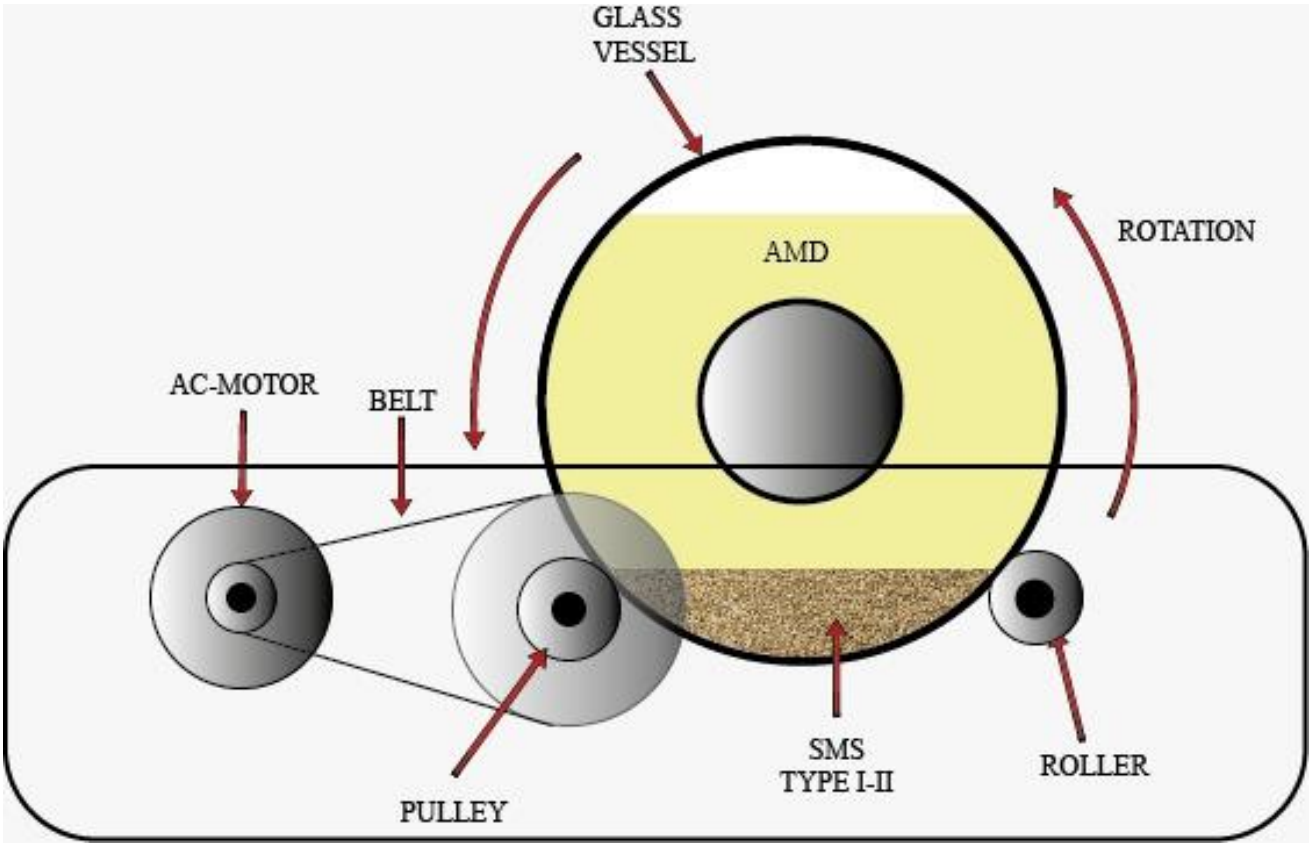

Fig. 2. Scheme of the rotational mixing device used in this work. The glass drum used to contain a 5:1 ratio of AMD (in yellow) and SMS (in brown) samples was supported on a series of bearings driven by an alternating current (AC) motor.

Table I. Physicochemical parameters of the AMD used in this work and maximum concentration values according to Colombian standards.

Parameter	Unit	Value	Resolution 0631 of 2015
Sulfates (SO_4^{2-})	$mg{\cdot}L^{-1}$	9418.75	1200 $mg{\cdot}L^{-1}$
Iron (Total Fe = Fe^{2+}, Fe^{3+})	$mg{\cdot}L^{-1}$	5426.67	2 $mg{\cdot}L^{-1}$
Arsenic (As)	$mg{\cdot}L^{-1}$	4.98	0,1 $mg{\cdot}L^{-1}$
pH	---	2.25	6.0 – 9.0
Dissolved oxygen (DO)	$mg{\cdot}L^{-1}$	0.70	N.A.
Cadmium (Cd^{2+})	$mg{\cdot}L^{-1}$	0.22	0,05 $mg{\cdot}L^{-1}$
Lead (Pb^{2+})	$mg{\cdot}L^{-1}$	0.03	0,2 $mg{\cdot}L^{-1}$

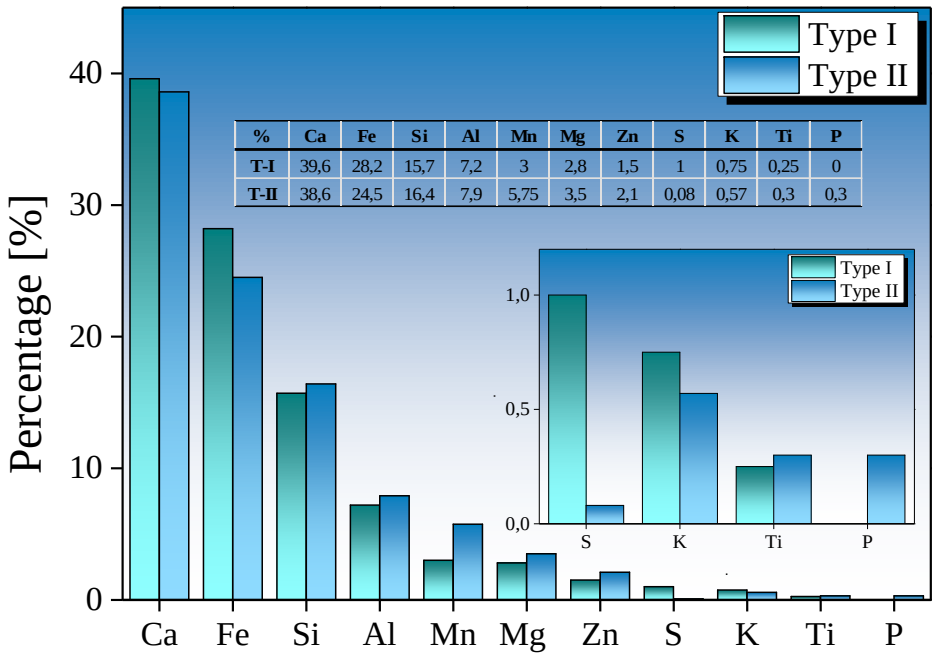

%	Ca	Fe	Si	Al	Mn	Mg	Zn	S	K	Ti	P
T-I	39,6	28,2	15,7	7,2	3	2,8	1,5	1	0,75	0,25	0
T-II	38,6	24,5	16,4	7,9	5,75	3,5	2,1	0,08	0,57	0,3	0,3

Fig. 3. Chemical composition of the Type-I (in green) and Type-II (in blue) BOF-SMS used in this work. The values were obtained by XRF technique.

3.2. AMD and SMS characterization.

Fig. 4 presents the pH behavior determined for the treated AMD, as a function of agitation and retention time, for periods of 12, 24 and 36 hours. The AMD treated samples with Type II SMS show a more significant increase in pH, reaching a value of 7.7 after 36 hours of treatment, compared to pH = 5.79 obtained in treated samples with Type I SMS.

The removal percentage of SO_4^{2-} and total Fe obtained in the treated AMD samples is presented in Fig. 5. The highest removal degree for SO_4^{2-} and total Fe was observed in the first 12 hours of treatment. The application of Type II SMS allows a higher removal than Type I SMS, reaching a sulfate (SO_4^{2-}) removal of 82.48 % and total Fe removal of 99.98 % at 12 hours of treatment. Although removal percentages of 69.39 % and 98.16 % for sulfates and total Fe were obtained in samples treated with Type I SMS.

The samples treated with Type II SMS achieved total Fe removal after 36 hours, while the total SO_4^{2-} removal was 85.13 %, exceeding the values previously reported by other authors, with values ranging between 50 % – 85 % (Masindi et al., 2020; Name & Sheridan, 2014; Zvimba et al., 2017). The total removal of heavy metals such as $As^{3+,\,5+}$, Cd^{2+}, and Pb^{2+} was obtained during 12 hours of treatment.

The removal percentage of SO_4^{2-} and total Fe obtained in the treated AMD samples is presented in Fig. 5. The highest removal degree for SO_4^{2-} and total Fe was observed in the first 12 hours of treatment. The application of Type II SMS allows a higher removal than Type I SMS, reaching a sulfate (SO_4^{2-}) removal of 82.48 % and total Fe removal of 99.98 % at 12 hours of treatment. Although removal percentages of 69.39 % and 98.16 % for sulfates and total Fe were obtained in samples treated with Type I SMS.

The samples treated with Type II SMS achieved total Fe removal after 36 hours, while the total SO_4^{2-} removal was 85.13 %, exceeding the values previously reported by other authors, with values ranging between 50 % – 85 % (Masindi et al., 2020; Name & Sheridan, 2014; Zvimba et al., 2017). The total removal of heavy metals such as $As^{3+,\,5+}$, Cd^{2+}, and Pb^{2+} was obtained during 12 hours of treatment.

The SMS used during 36 hours of AMD treatment were analyzed by XRF technique to determine chemical composition variation. The results are presented in Fig. 6 for AMD samples treated with a Type I SMS and Fig. 7 for AMD samples treated with a Type II SMS. A percentage reduction in Ca and Mg content of 23.8 % and 3.5 % for Type I samples and 8.8 % and 3.0 % for Type II samples, respectively, is observed. The release of these elements in solution is related to a pH increase observed in AMD treated samples due to their dissolution in the form of cations and $(OH)^-$ radicals, which increase alkalinity solution (Name & Sheridan, 2014; Reardon et al., 1995). The dissolution of basic cations and formation of $(OH)^-$ radicals are determined by the following chemical reactions as show in Equations 5, 6, and 7:

$$MgO + H_2O \rightarrow Mg^{2+} + 2OH^- \quad (5)$$

$$CaO + H_2O \rightarrow Ca^{2+} + 2OH^- \quad (6)$$

$$MnO_2 + 2H_2O \rightarrow Mn^{4+} + 4OH^- \quad (7)$$

The pH rise in treated AMD samples reveals that elements such as Ca^{2+}, Mn^{4+}, and Mg^{2+} contained in the SMS are available in solution, even at low pH, favoring the release of OH^- radicals in solution producing alkalinity (Akinwekomi et al., 2017; Feng et al., 2004; Masindi et al., 2018; Rose, 2010). The AMD samples treated with Type I SMS show a lower pH increase compared to the samples treated with the Type II SMS. This is explained by insufficient kinetics reaction to reach a neutrality value (pH = 7.0) (Rose, 2010). The alkalinity produced from the addition of Type I SMS is counteracted by the high acidity production within the AMD, limiting the pH increase.

The higher efficiency in pH increases when using Type II SMS presumes that applying a larger contact area offered by smaller particle size favors the physicochemical reactions, which contributes to a more reactive surface in contact with the AMD. The SMS size and AMD neutralization depend on SMS particle size and SMS chemical composition. The larger particles provide less surface area which in turn give less reaction time and alkalinity production (Ziemkiewicz & Skousen, 1999).

The neutralization process and alkaline reagent size relation (surface area) were observed as well for other alkaline materials such as calcite. It was determined that the rate of neutralization is directly related to the dosage of $CaCO_3$, influenced by the particle size (the finer particle, the higher the rate of neutralization)(Maree & Plessis, 1993). Furthermore, these basic cations and $(OH)^-$ radicals are also required to form insoluble compounds (precipitate formation) (Feng et al., 2004; Jeong et al., 2016; Kang et al., 2019; Rose, 2010; Wang et al., 2019). A part of the radicals is destined for the formation of Fe hydroxides from AMD and SMS (Name & Sheridan, 2014).

An increase in Fe, Si, and S content was observed in Type I SMS samples, with a contribution in the concentration of 23.4 %, 2.3 %, and 5.17 %, respectively; while the increase in Fe, Si, and S content in Type II SMS was 4 %, 4.5 %, and 1.6 %. The increase in S and Fe values is mainly due to the absorption of SO_4^{2-} and total Fe ions initially present in the AMD samples, favoring the formation of new mineral phases on the SMS surface. In contrast, an increase in Si content may be related to the high degradation of the mineralogical phases that compose the other metals, as mentioned above, allowing higher Si values in the SMS used in AMD treatment stages. Due to the reduced treatment time used in this work and a higher reactivity of the calcium compounds, the slow dissolution of the silica-rich glass present in the SMS is not noticeable. Hence, its contribution to the pH decrease is not significant (Doye & Duchesne, 2003).

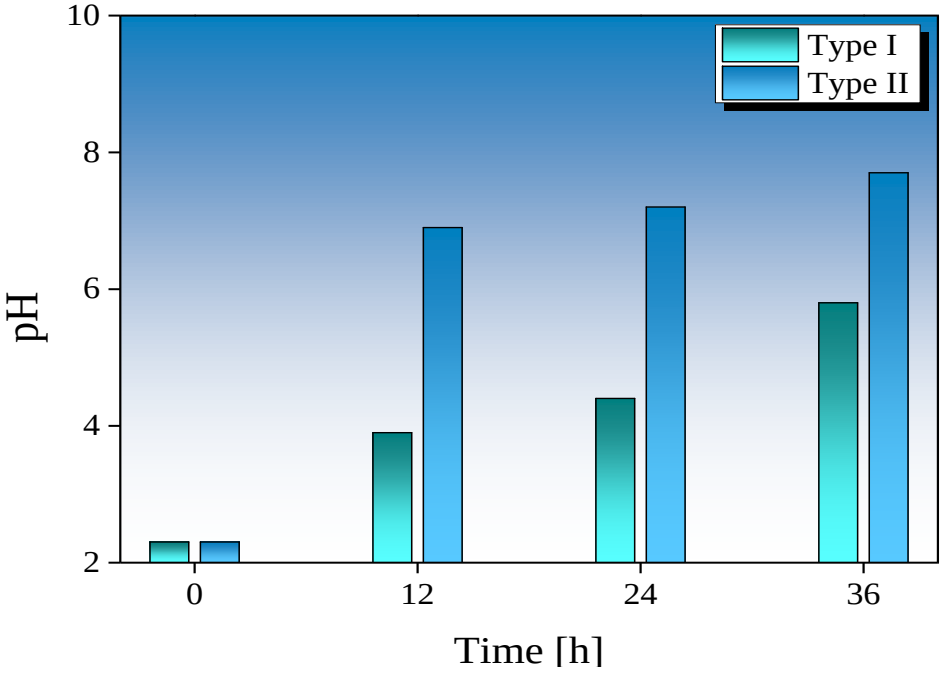

Fig. 4. Relationship between the pH in AMD samples and the treatment time using a Type-I (in green) and Type-II (in blue) BOF-SMS used in this work.

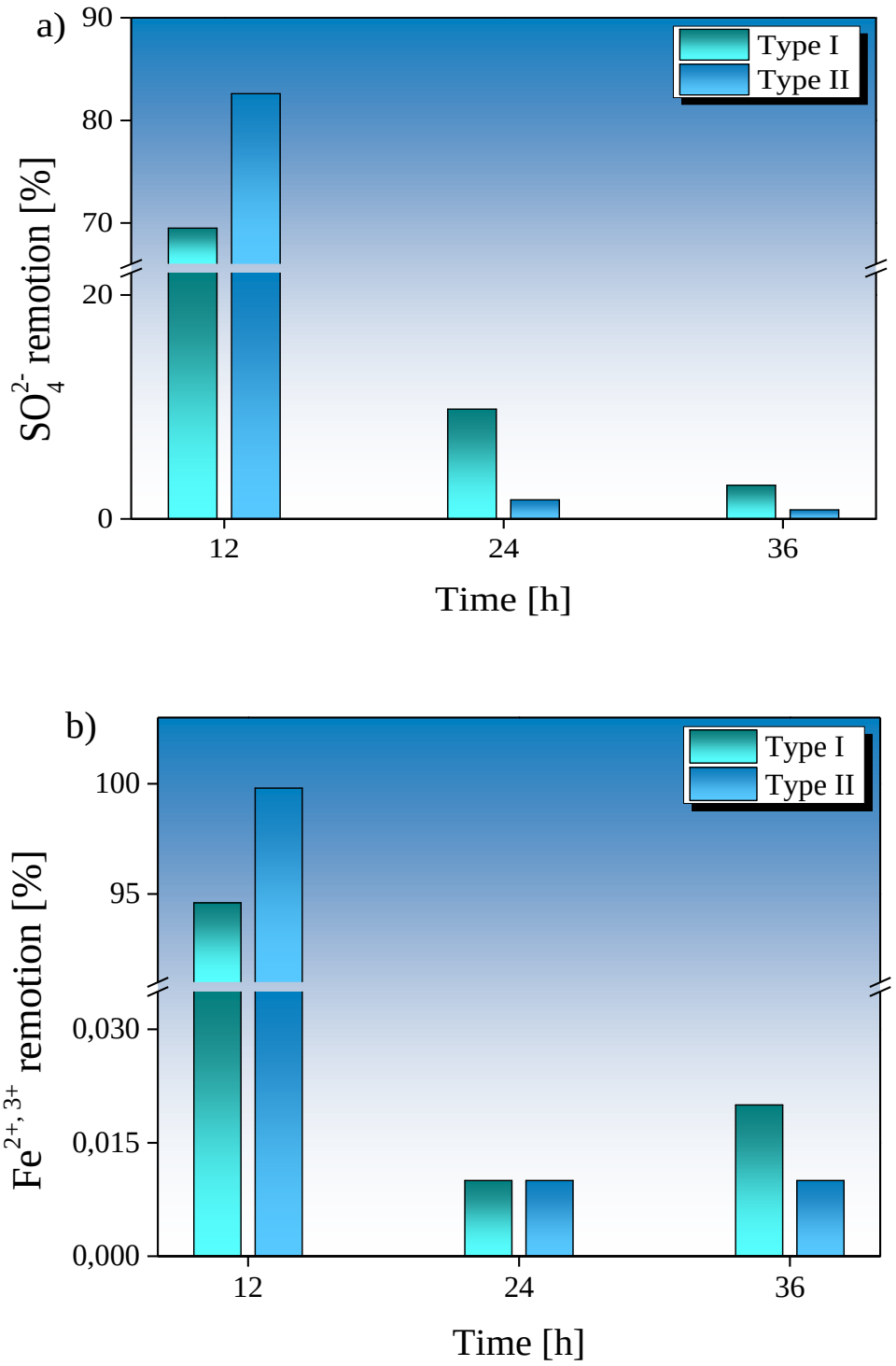

Fig. 5. Behavior of the SO_4^{2-} and Fe removal percentage in relation to the treatment time of AMD samples treated with Type I (in green) and Type II (in blue) BOF-SMS.
In a) SO_4^{2-} and b) Fe removal percentage obtained at 12 h, 24 h, and 36 h of treatment.

The Ca and Mg dissolution degree in Ca^{2+} and Mg^{4+} in Type II SMS samples was lower than observed in the Type I SMS samples. However, the increase in pH in AMD samples treated with Type II SMS was significantly higher. This behavior implies greater control and efficiency in the reaction and stability of the precipitates formed, allowing for a more significant contribution of (OH)-radicals that favor increased pH values. The insoluble iron precipitates produced from the interaction of $(OH)^-$ radicals and Fe^{3+} present in the AMD gradually is adhered to the SMS, forming a shielding or coating evidenced by an increase of Fe in the final chemical composition of the SMS. The formation of $Fe(OH)_3$ can generate a high protonic acidity (H^+) load associated with hydrolytic reactions, as shown in Equations 8 and 9 (Franti ,1998; Zipper et al., 2014), which may have contributed to a lower degree of Fe removal and a low increase in pH in samples treated with Type I SMS.

$$Fe^{3+} + 3H_2O \rightarrow Fe(OH)_3 + 3H^+ \quad (8)$$

$$Fe^{+2} + HCO_3^- \rightarrow FeCO_3 + H^+ \quad (9)$$

Both Types of SMS present an increase in S content, which possibly is associated with gypsum and hydroxide-sulfates formation over SMS surface (Bigham et al., 1996; Duchesne & Reardon, 1998). Gypsum and $Fe(OH)_3$ precipitates can adhere to the SMS surface during formation, and this coating layer can trap other contaminants such as $As^{3+, 5+}$, Cd^{2+}, and Pb^{2+} during the rotational process. (Roza Llera et al., 2021; Satti et al., 2020). The AMD high Fe concentration and the presence of $Fe(OH)_3$ precipitates in the solution may also favor arsenic removal through the possible formation of ferric arsenates.

This behavior has been previously reported for other dissolved metals presents in AMD (Doye & Duchesne, 2003; Farrell & Chaudhary, 2013). Adsorption processes removed dissolved heavy metals completely from AMD because the pH increase was not high enough for their removal by precipitation formation (Matlock et al., 2002; Petrilakova et al., 2014; Vasquez & Escobar, 2020; Zhang et al., 2018). The solubility of SO_4^{2-}, present in the AMD, is controlled by gypsum precipitation (Geldenhuys et al., 2003); which begins its formation and precipitation process at low pH, where it has been reported that the precipitation process begins at pH > 3.75 (Gitari et al., 2008; Macías et al., 2017; Madzivire et al., 2011).

The rotational mixing device works as a conventional autogenous grinding process (Wills, 1988). Abrasion is generated between the SMS particles, favoring some detachment of precipitates that coat the surface, exposing the reactive surface of the SMS again to the acid medium. The application of rotational mixing devices would allow a more extended period of operation, reducing the cleaning stages required in the mechanisms conventionally used for the treatment of AMD.

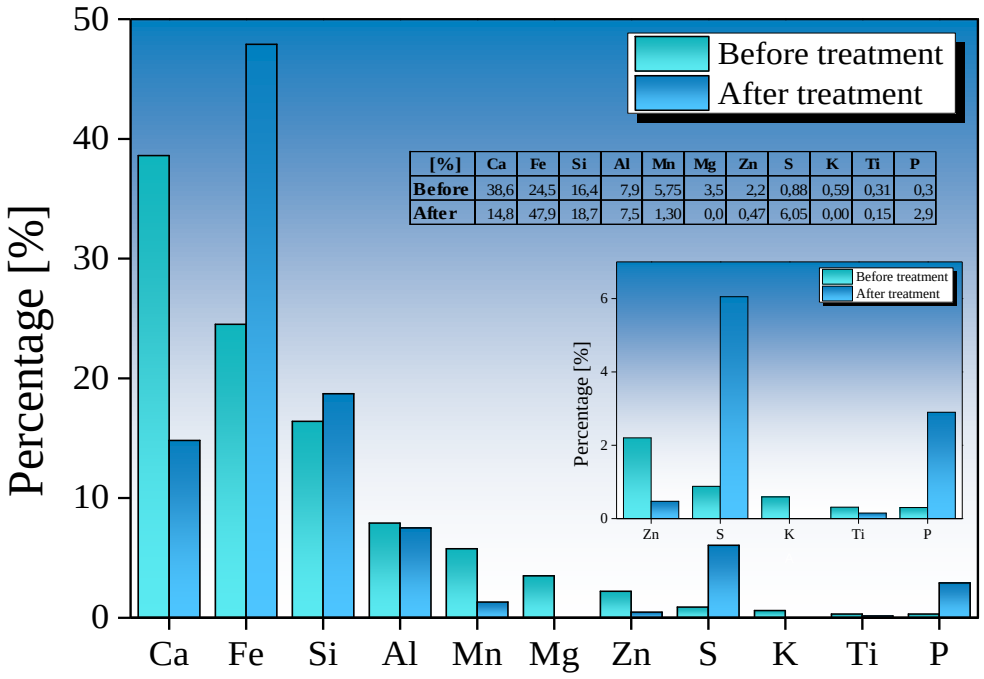

Fig. 6. Chemical variation before (in green) and after (in blue) the treatment of AMD samples by applying a Type I BOF-SMS in a rotational mixing device.

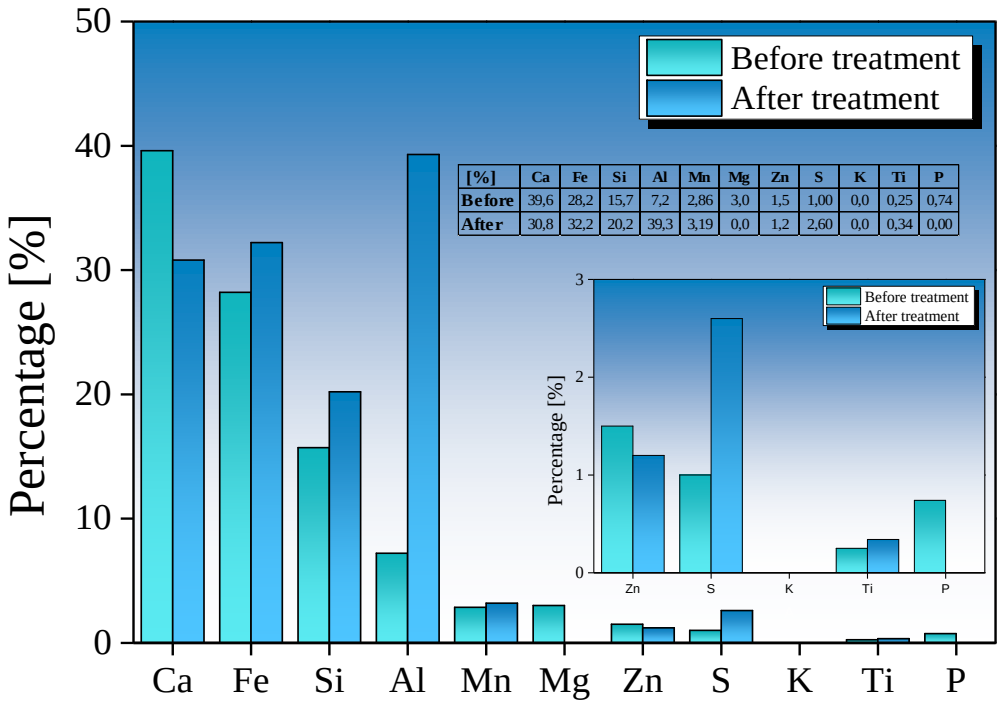

Fig. 7 Chemical variation before (in green) and after (in blue) the treatment of AMD samples by applying a Type II BOF-SMS in a rotational mixing device.

4. Conclusions

In the present work, the effect of the particle size of SMS produced in BOF type converter furnaces in a steel plant for the treatment of acid mine drainage (AMD) produced in the region of Boyacá, Colombia, was studied. The tests were carried out using two types of slag particle size, which were added to the AMD samples for treatment in a rotational mixing device during different time intervals.

The results obtained in this research work showed that SMS application with a smaller particle size allows a larger reactive contact area with the AMD. This behavior allows a higher ion exchange rate, resulting in a pH increase and the precipitation of sulfates and total Fe dissolved in the AMD. The total heavy metals removal present in AMD during the first 12 hours of treatment demonstrates that this process could have been generated by absorbing mineral phases such as gypsum and $Fe(OH)_3$ during the formation and growth process. The elimination of heavy metals by precipitation process is completely discarded because a high pH is not achieved where the insolubilization of these metals begins. The pH variation obtained for the treated AMD samples is a function of alkalinity production by the SMS slag. Low AMD pH values (< 7.0) reveal low alkalinity production, and heavy metals precipitation under this condition is not achieved by their low solubility. Alkalinity production depends on the SMS slag chemical composition, and the particle size, as mentioned in the literature.

Although, both types of SMS demonstrated an optimum performance in removing sulfates, total Fe, and heavy metals. Type II SMS showed a more significant increase in pH values in shorter time intervals, a fundamental aspect of their industrial application. In addition, applying a rotational mixing system allows some abrasion and detachment of the precipitates adhered on the slag surface, maintaining the medium's reactivity and AMD treatment. In this work, the abrasion process and the detachment of precipitates formed on the surface of SMS slag particles were not analyzed. However, it will be necessary to understand how the mixing process influences compounds' formation, such as gypsum and $Fe(OH)_3$, and how these chemical species remove heavy metals at low pH (< 7.0). This situation is going to be analyzed in the near future.

Considering that SMS is used as aggregates in construction, this waste material has the potential of being previously used in the AMD treatment and then confined within the concrete or asphalt, reducing the toxicological risk that these heavy metals represent in the environment. It would be necessary to evaluate how gypsum and $Fe(OH)_3$ coatings influence these materials' quality, final strength, and

durability. The authors show their interest in applying this type of device at pilot and industrial scale to treat AMD produced in the mining region of the department of Boyacá, Colombia.

Conflict of interest

The authors have no conflict of interest to declare.

Acknowledgements

The authors wish thanking to the Faculty of Engineering of the Pedagogical and Technological University of Colombia - UPTC for supporting this work. One of the authors (N.R.A), appreciates the invitation from these institutions to participate and contribute to the development of this work.

References

Akinwekomi, V., Maree, J. P., Zvinowanda, C., & Masindi, V. (2017). Synthesis of magnetite from iron-rich mine water using sodium carbonate. *Journal of Environmental Chemical Engineering*, *5*(3), 2699–2707. https://doi.org/10.1016/j.jece.2017.05.025

Aziz, M. M. A., Hainin, M. R., Yaacob, H., Ali, Z., Chang, F.-L., & Adnan, A. M. (2014). Characterisation and utilisation of steel slag for the construction of roads and highways. *Materials Research Innovations*, *18*(sup6), S6-255-S6-259. https://doi.org/10.1179/1432891714Z.000000000967

Belhadj, E., Diliberto, C., & Lecomte, A. (2012). Characterization and activation of Basic Oxygen Furnace slag. *Cement and Concrete Composites*, *34*(1), 34–40. https://doi.org/10.1016/j.cemconcomp.2011.08.012

Bigham, J. M., Schwertmann, U., Traina, S. J., Winland, R. L., & Wolf, M. (1996). Schwertmannite and the chemical modeling of iron in acid sulfate waters. *Geochimica et Cosmochimica Acta*, *60*(12), 2111–2121. https://doi.org/10.1016/0016-7037(96)00091-9

Bing, L., Biao, T., Zhen, M., Hanchi, C., & Hongbo, L. (2019). Physical and Chemical Properties of Steel Slag and Utilization Technology of Steel Slag at Home and Abroad. *IOP Conference Series: Earth and Environmental Science*, *242*(3), 4–9. https://doi.org/10.1088/1755-1315/242/3/032012

Bwapwa, J. K., Jaiyeola, A. T., & Chetty, R. (2017). Bioremediation of acid mine drainage using algae strains: A review. *South African Journal of Chemical Engineering*, *24*, 62–70. https://doi.org/10.1016/j.sajce.2017.06.005

Clyde, E. J., Champagne, P., Jamieson, H. E., Gorman, C., & Sourial, J. (2016). The use of a passive treatment system for the mitigation of acid mine drainage at the Williams Brothers Mine (California): pilot-scale study. *Journal of Cleaner Production*, *130*, 116–125. https://doi.org/10.1016/j.jclepro.2016.03.145

Dold, B. (2014). Evolution of acid mine drainage formation in sulphidic mine tailings. *Minerals*, *4*(3), 621–641. https://doi.org/10.3390/min4030621

Doye, I., & Duchesne, J. (2003). Neutralisation of acid mine drainage with alkaline industrial residues: laboratory investigation using batch-leaching tests. *Applied Geochemistry*, *18*(8), 1197–1213. https://doi.org/10.1016/S0883-2927(02)00246-9

Duchesne, J., & Reardon, E. J. (1998). Determining controls on element concentrations in cement kiln dust leachate. *Waste Management*, *18*(5), 339–350. https://doi.org/10.1016/S0956-053X(98)00078-6

Farrell, J., & Chaudhary, B. K. (2013). Understanding Arsenate Reaction Kinetics with Ferric Hydroxides. *Environmental Science & Technology*, *47*(15), 8342–8347. https://doi.org/10.1021/es4013382

Feng, D., van Deventer, J. S. J., & Aldrich, C. (2004). Removal of pollutants from acid mine wastewater using metallurgical by-product slags. *Separation and Purification Technology*, *40*(1), 61–67. https://doi.org/10.1016/j.seppur.2004.01.003

Franti, D. J. (1998). *Acid mine drainage treatment in an open limestone channel emphasizing aeration & retention* (Doctoral dissertation, Montana State University-Bozeman, College of Agriculture). https://scholarworks.montana.edu/xmlui/handle/1/7809

Geldenhuys, AJ, Maree, JP, De Beer, M. & Hlabela, P. (2003). An integrated limestone/lime process for partial sulphate removal. *Journal of the Southern African Institute of Mining and Metallurgy*, *103*(6), 345-353. https://hdl.handle.net/10520/AJA0038223X_2806

Gitari, W. M., Petrik, L. F., Etchebers, O., Key, D. L., & Okujeni, C. (2008). Utilization of fly ash for treatment of coal mines wastewater: Solubility controls on major inorganic contaminants. *Fuel*, *87*(12), 2450–2462. https://doi.org/10.1016/j.fuel.2008.03.018

Hallberg, K. B. (2010). New perspectives in acid mine drainage microbiology. *Hydrometallurgy*, *104*(3–4), 448–453. https://doi.org/10.1016/j.hydromet.2009.12.013

Hustwit, C. C., Ackman, T. E., & Erickson, P. M. (1992). Role of oxygen transfer in acid mine drainage treatment. *Environment Science Chemistry*, *USBM*, *USDI RI 9405*.

IDEAM. (2018). Instituto de Hidrología, Meteorología y Estudios Ambientales. *Tiempo y clima, Reportes*. *Boletín Climatológico*. http://www.ideam.gov.co/web/tiempo-y-clima/climatologico-mensual/-/document_library_display/xYvlPc4uxk1Y/view/71473013

IDEAM. (2020). Instructivo de toma y preservación de muestras sedimentos y agua superficial para la red de monitoreo de calidad del IDEAM.

Jeong, Y., Eun, J., Jun, Y., Park, J., & Ha, J. (2016). Influence of four additional activators on hydrated-lime [Ca (OH) 2] activated ground granulated blast-furnace slag. *Cement and Concrete Composites*, *65*, 1–10. https://doi.org/10.1016/j.cemconcomp.2015.10.007

Kang, S., Kwon, Y., Hong, S., & Chun, S. (2019). Hydrated lime activation on byproducts for eco-friendly production of structural mortars. *Journal of Cleaner Production*, *231*, 1389–1398. https://doi.org/10.1016/j.jclepro.2019.05.313

Kobielska, P. A., Howarth, A. J., Farha, O. K., & Nayak, S. (2018). Metal–organic frameworks for heavy metal removal from water. *Coordination Chemistry Reviews*, *358*, 92–107. https://doi.org/10.1016/j.ccr.2017.12.010

Król, A., Mizerna, K., & Bożym, M. (2020). *An assessment of pH-dependent release and mobility of heavy metals from metallurgical slag*. *Journal of hazardous materials*, *384*, 121502. https://doi.org/10.1016/j.jhazmat.2019.121502

Luptáková, A., Mačingová, E., Kotuličová, I., & Rudzanová, D. (2016). Sulphates Removal from Acid Mine Drainage. *IOP Conference Series: Earth and Environmental Science*, *44*(5), 052040. https://doi.org/10.1088/1755-1315/44/5/052040

Macías, F., Pérez-López, R., Caraballo, M. A., Cánovas, C. R., & Nieto, J. M. (2017). Management strategies and valorization for waste sludge from active treatment of extremely metal-polluted acid mine drainage: A contribution for sustainable mining. *Journal of Cleaner Production*, *141*, 1057–1066. https://doi.org/10.1016/j.jclepro.2016.09.181

Madzivire, G., Gitari, W. M., Vadapalli, V. R. K., Ojumu, T. V., & Petrik, L. F. (2011). Fate of sulphate removed during the treatment of circumneutral mine water and acid mine drainage with coal fly ash: Modelling and experimental approach. *Minerals Engineering*, *24*(13), 1467–1477. https://doi.org/10.1016/j.mineng.2011.07.009

Maree, J. P., & Plessis, P. D. (1993). Neutralisation of acidic effluents with limestone. In Water Research Commission.

Masindi, V., Ramakokovhu, M. M., Osman, M. S., & Tekere, M. (2020). Advanced application of BOF and SAF slags for the treatment of acid mine drainage (AMD): a comparative study. *Materials Today: Proceedings*, *38*, 934-941. https://doi.org/10.1016/j.matpr.2020.05.422

Masindi, V. (2016). A novel technology for neutralizing acidity and attenuating toxic chemical species from acid mine drainage using cryptocrystalline magnesite tailings. *Journal of Water Process Engineering*, *10*, 67-77. https://doi.org/10.1016/j.jwpe.2016.02.002

Masindi, V., Gitari, M. W., Tutu, H., & DeBeer, M. (2017). Synthesis of cryptocrystalline magnesite–bentonite clay composite and its application for neutralization and attenuation of inorganic contaminants in acidic and metalliferous mine drainage. *Journal of water process engineering*, *15*, 2-17. https://doi.org/10.1016/j.jwpe.2015.11.007

Masindi, V., Osman, M. S., & Abu-Mahfouz, A. M. (2017). Integrated treatment of acid mine drainage using BOF slag, lime/soda ash and reverse osmosis (RO): Implication for the production of drinking water. *Desalination*, *424*, 45-52. https://doi.org/10.1016/j.desal.2017.10.002

Masindi, V., Osman, M. S., Mbhele, R. N., & Rikhotso, R. (2018). Fate of pollutants post treatment of acid mine drainage with basic oxygen furnace slag: Validation of experimental results with a geochemical model. *Journal of Cleaner Production*, *172*, 2899-2909. https://doi.org/10.1016/j.jclepro.2017.11.124

Matlock, M. M., Howerton, B. S., & Atwood, D. A. (2002). Chemical precipitation of heavy metals from acid mine drainage. *Water Research*, *36*(19), 4757–4764. https://doi.org/10.1016/S0043-1354(02)00149-5

Name, T., & Sheridan, C. (2014). Remediation of acid mine drainage using metallurgical slags. *Minerals Engineering*, *64*, 15–22. https://doi.org/10.1016/j.mineng.2014.03.024

Núñez-Gómez, D., Rodrigues, C., Lapolli, F. R., & Lobo-Recio, M. Á. (2019). Adsorption of heavy metals from coal acid mine drainage by shrimp shell waste: Isotherm and continuous-flow studies. *Journal of Environmental Chemical Engineering*, *7*(1), 102787. https://doi.org/10.1016/j.jece.2018.11.032

Obreque-Contreras, J., Pérez-Flores, D., & Gutiérrez, P. (2015). Acid Mine Drainage in Chile: An Opportunity to Apply Bioremediation Technology. *Journal of Waste Water Treatment & Analysis*, *06*(03). https://doi.org/10.4172/2157-7587.1000215

Petrilakova, A., Balintova, M., & Holub, M. (2014). Precipitation of heavy metals from acid mine drainage and their geochemical modeling. *Selected Scientific Papers - Journal of Civil Engineering*, *9*(1), 79–86. https://doi.org/10.2478/sspjce-2014-0009

Prieto, G., & Duitama, L. M. (2004). Acid Drainage of Coal Mining in Cundinamarca Department, Colombia. In *Environmental Geochemistry in Tropical and Subtropical Environments* (pp. 125–134). Springer Berlin Heidelberg. https://doi.org/10.1007/978-3-662-07060-4_11

Rambabu, K., Banat, F., Pham, Q. M., Ho, S.-H., Ren, N.-Q., & Show, P. L. (2020). Biological remediation of acid mine drainage: Review of past trends and current outlook. *Environmental Science and Ecotechnology*, *2*, 100024. https://doi.org/10.1016/j.ese.2020.100024

Reardon, E., Czank, C., Warren, C., Dayal, R., Jonsthon, H. (1995). Determining controls on element concentrations in fly ash leachate. *Waste Management & Research*, *13*(5), 435–450. https://doi.org/10.1016/S0734-242X(05)80023-0

Resolución 631 de 2015. (2015*)*. Ministerio de Medio Ambiente y Desarrollo Sostenible - Colombia. (p. 13). (2105).

Rojas Arias, N., Perez Villamil, F. R., & Arango Patermina, H. J. (2018). Effect of particle size in the reduction of lateritic Ni ore in a Linder reactor. *Revista ION*, *31*(1), 97–104. https://doi.org/10.18273/revion.v31n1-2018015

Rose, A. W. (2010). Advance in passive treatment of coal mine drainage 1989-2009. *Barnhisel, R.I. (Ed), Joint Mining Reclamation Conference. ASMR, Lexington, KY.*, 847. https://www.asrs.us/Portals/0/Documents/Conference-Proceedings/2010/0847-Rose.pdf

Roza Llera, A., Jimenez, A., & Fernández-Díaz, L. (2021). Removal of Pb from Water: The Effectiveness of Gypsum and Calcite Mixtures. *Minerals*, *11*(1), 66. https://doi.org/10.3390/min11010066

Satti, Z., Akhtar, M., Mazhar, N., Khan, S. U., Ahmed, N., Yasir, Q. M., ... & Ahmad, W. (2020). Adsorption of cadmium from aqueous solution onto untreated gypsum rock material: Equilibrium and kinetics. *Biointerface Res. Appl. Chem*, *11*, 10755-10764. https://doi.org/10.33263/BRIAC113.1075510764

Silva, L. F. O., Hower, J. C., Dotto, G. L., Oliveira, M. L. S., & Moreno, A. L. (2020). Nanoparticles from evaporite materials in Colombian coal mine drainages. *International Journal of Coal Geology*, *230*, 103588. https://doi.org/10.1016/j.coal.2020.103588

Skousen, J., Zipper, C., Rose, A., Ziemkiewicz, P., Nairn, R., McDonald, L. M., & Kleinmann, R. L. (2017). Review of passive systems for acid mine drainage treatment. *Mine Water and the Environment*, *36*, 133–153. https://doi.org/10.1007/s10230-016-0417-1

Skousen, J. G., Sexstone, A., & Ziemkiewicz, P. F. (2000). Acid mine drainage control and treatment. *Reclamation of drastically disturbed lands*, *American Society of Agronomy, 41*, 131-168. https://doi.org/10.2134/agronmonogr41.c6

Skousen, Jeff, & Ziemkiewicz, P. (2005). Performance of 116 passive treatment systems for acid mine drainage. *Journal American Society of Mining and Reclamation*, *2005*(1), 1100–1133. https://doi.org/10.21000/JASMR05011100

Skousen, Jeffrey G., Ziemkiewicz, P. F., & McDonald, L. M. (2019). Acid mine drainage formation, control and treatment: Approaches and strategies. *Extractive Industries and Society*, *6*(1), 241–249. https://doi.org/10.1016/j.exis.2018.09.008

Tabelin, C. B., Sasaki, R., Igarashi, T., Park, I., Tamoto, S., Arima, T., ... & Hiroyoshi, N. (2017). Simultaneous leaching of arsenite, arsenate, selenite and selenate, and their migration in tunnel-excavated sedimentary rocks: I. Column experiments under intermittent and unsaturated flow. *Chemosphere*, *186*, 558-569. https://doi.org/10.1016/j.chemosphere.2017.07.145

Taylor, J., Pape, S., & Murphy, N. (2005). A summary of passive and active treatment technologies for acid and metalliferous drainage (AMD). In Proceedings of the 5th Australian workshop on acid drainage (Vol. 29, pp. 1-49).

Thomas, C., Rosales, J., Polanco, J. A., & Agrela, F. (2019). Steel slags. In *New Trends in Eco-efficient and Recycled Concrete* (pp. 169–190). Elsevier. https://doi.org/10.1016/B978-0-08-102480-5.00007-5

Tiwari, M., Bajpai, D. S., & Dewangan, D. U. (2016). Steel Slag Utilization — Overview in Indian Perspective. *International Journal of Advanced Research*, *4*(8), 2232–2246. https://doi.org/10.21474/IJAR01/1442

Van der Sloot, H. A., & Van Zomeren, A. (2012). Characterisation Leaching Tests and Associated Geochemical Speciation Modelling to Assess Long Term Release Behaviour from Extractive Wastes. *Mine Water and the Environment*, *31*(2), 92–103. https://doi.org/10.1007/s10230-012-0182-8

Vasquez, O. Y., & Escobar, M. C. (2020). Reactores Bioquímicos Pasivos: Una alternativa biotecnológica para la remediación de drenajes ácidos de mina. *Revista Colombiana de Biotecnología*, *22*(2), 53–69. https://doi.org/10.15446/rev.colomb.biote.v22n2.74090

Wang, L., Cho, D., Tsang, D. C. W., Cao, X., Hou, D., Shen, Z., Alessi, D. S., Sik, Y., & Sun, C. (2019). Green remediation of As and Pb contaminated soil using cement-free clay- based stabilization / solidification. *Environment International*, *126* 336–345. https://doi.org/10.1016/j.envint.2019.02.057

Wills, B. A. (1988). Grinding Mills. In *Mineral Processing Technology* (pp. 253–308). Elsevier. https://doi.org/10.1016/B978-0-08-034937-4.50016-8

Wolfe, D. (2015). Effective Ranges of a Modeled Open Limestone Channel. *SIAM Undergraduate Research Online*, *8*, 160–176. https://doi.org/10.1137/15S013788

Zhang, Y., Zhang, H., Zhang, Z., Liu, C., Sun, C., Zhang, W., & Marhaba, T. (2018). pH Effect on Heavy Metal Release from a Polluted Sediment. *Journal of Chemistry*, *2018*, 1–7. https://doi.org/10.1155/2018/7597640

Ziemkiewicz, P., & Skousen, J. (1999). Steel Slag in Acid Mine Drainage Treatment and Control. *Journal American Society of Mining and Reclamation*, *1999*(1), 651–656. https://doi.org/10.21000/JASMR99010651

Zipper, C., Skousen, J., & Jage, C. (2014). Passive treatment of acid-mine drainage. *Powell River Project - Recklamation Guidelines For Surface Mined Land, 460–133*, 1–14. https://doi.org/10.1002/9781118749197.ch30

Zvimba, J. N., Siyakatshana, N., & Mathye, M. (2017). Passive neutralization of acid mine drainage using basic oxygen furnace slag as neutralization material: experimental and modelling. *Water Science and Technology*, *75*(5), 1014–1024. https://doi.org/10.2166/wst.2016.579